The CMS High Granularity Calorimeter for High Luminosity LHC

Rachel Yohay (Florida State University)
On behalf of the CMS Collaboration

15th Vienna Conference on Instrumentation

February 19, 2019

Outline

- Motivation
- Detector design
- Silicon sensor prototyping
- Performance
- Conclusions and outlook

Outline

- Motivation
- Detector design
- Silicon sensor prototyping
- Performance
- Conclusions and outlook

The focus of this talk

Motivation

http://cms.web.cern.ch/news/cms-detector-design

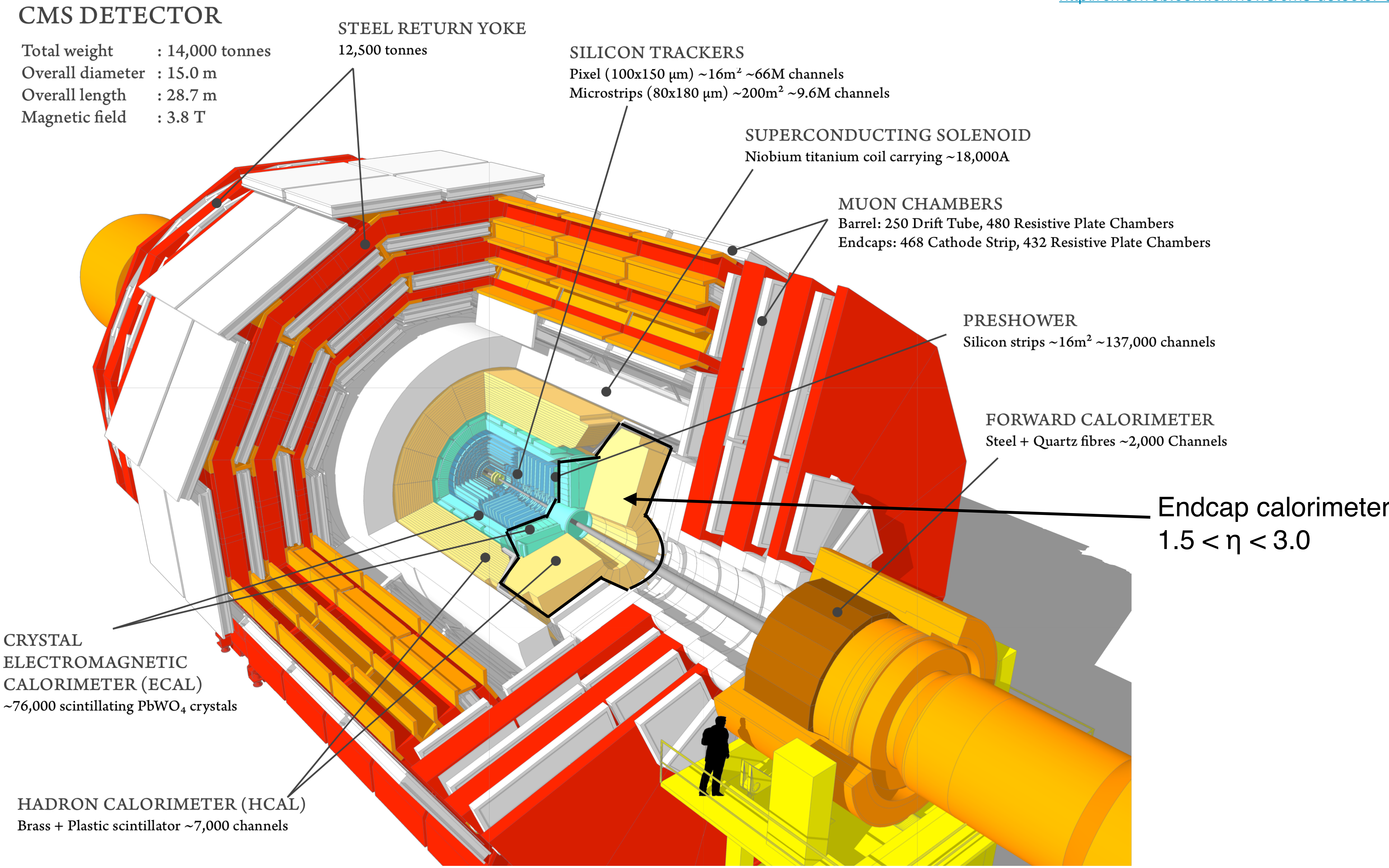

High luminosity physics and the endcap

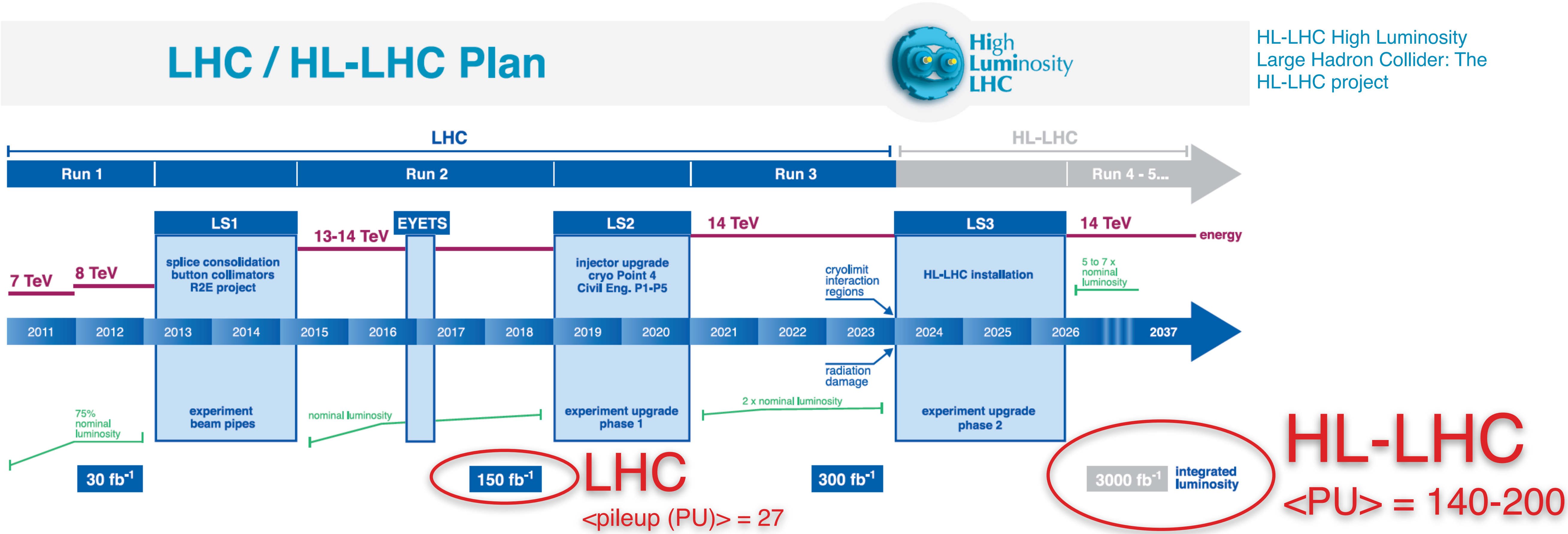

HL-LHC High Luminosity Large Hadron Collider: The HL-LHC project

- Physics goals of the High Luminosity LHC (HL-LHC) make specific performance demands of the endcap calorimeter
  - Measurement of **vector boson fusion** (VBF) Higgs production and **WW scattering**, processes identified by **two characteristic forward jets**
  - Searches for rare heavy particles associated with supersymmetry (SUSY) and other Standard Model (SM) extensions
    - Extend electron, photon, tau, and jet reconstruction to the endcaps to better exploit the dataset
    - Improved **missing transverse energy** (ME_T) reconstruction
- CMS upgrade philosophy: **equal or better performance under HL-LHC conditions**

Complete overhaul required

CERN-LHCC-2015-010

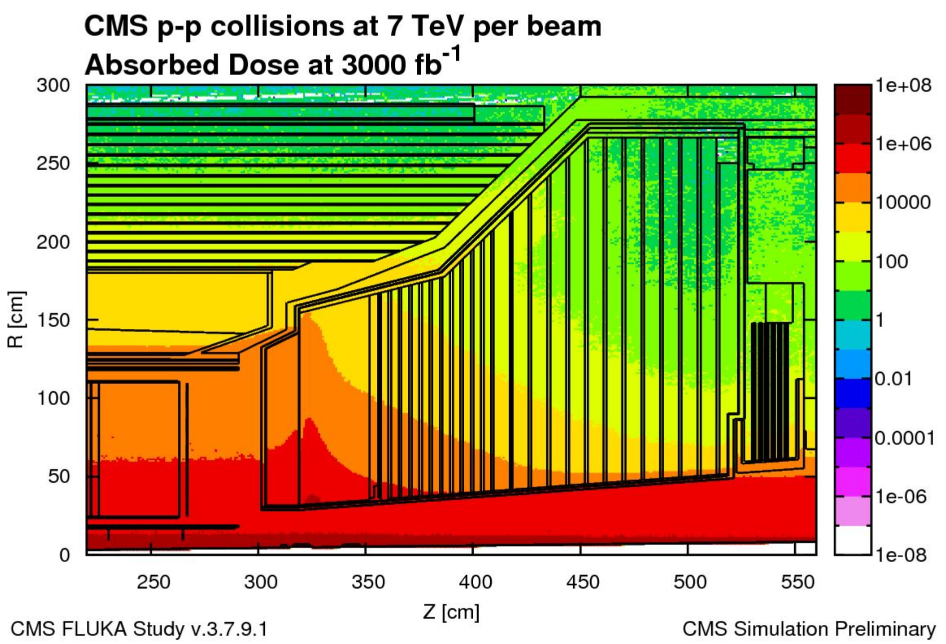

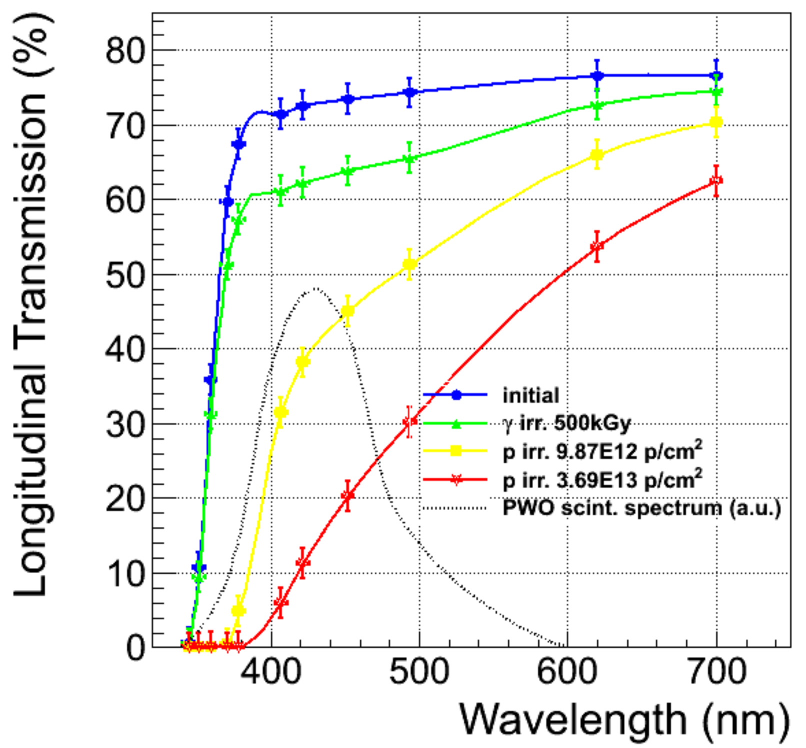

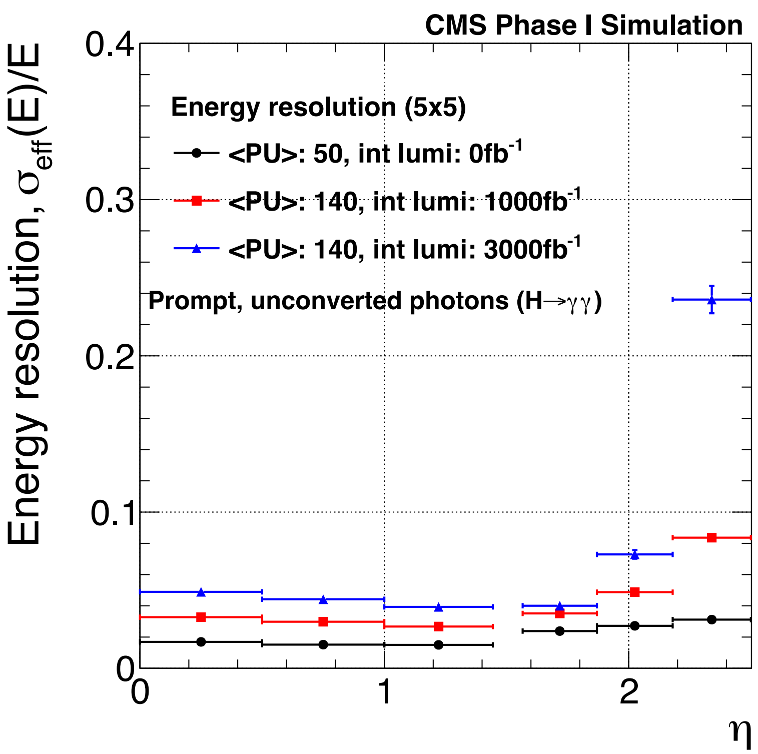

- $PbWO_4$ crystal transmission loss due to radiation damage
- Worsening energy resolution due to increased pileup

Detector design

High Granularity Calorimeter (CE)

CERN-LHCC-2017-023

Active Elements:

- Hexagonal modules based on Si sensors in CE-E and high-radiation regions of CE-H
- "Cassettes": multiple modules mounted on cooling plates with electronics and absorbers
- Scintillating tiles with SiPM readout in low-radiation regions of CE-H

Key Parameters:

- CE covers $1.5 < \eta < 3.0$
- ~215 tonnes per endcap
- Full system maintained at -30°C
- ~600m^2 of silicon sensors
- ~500m^2 of scintillators
- 6M si channels, 0.5 or 1 cm^2 cell size
- ~27000 si modules
- Power at end of HL-LHC: ~110 kW per endcap

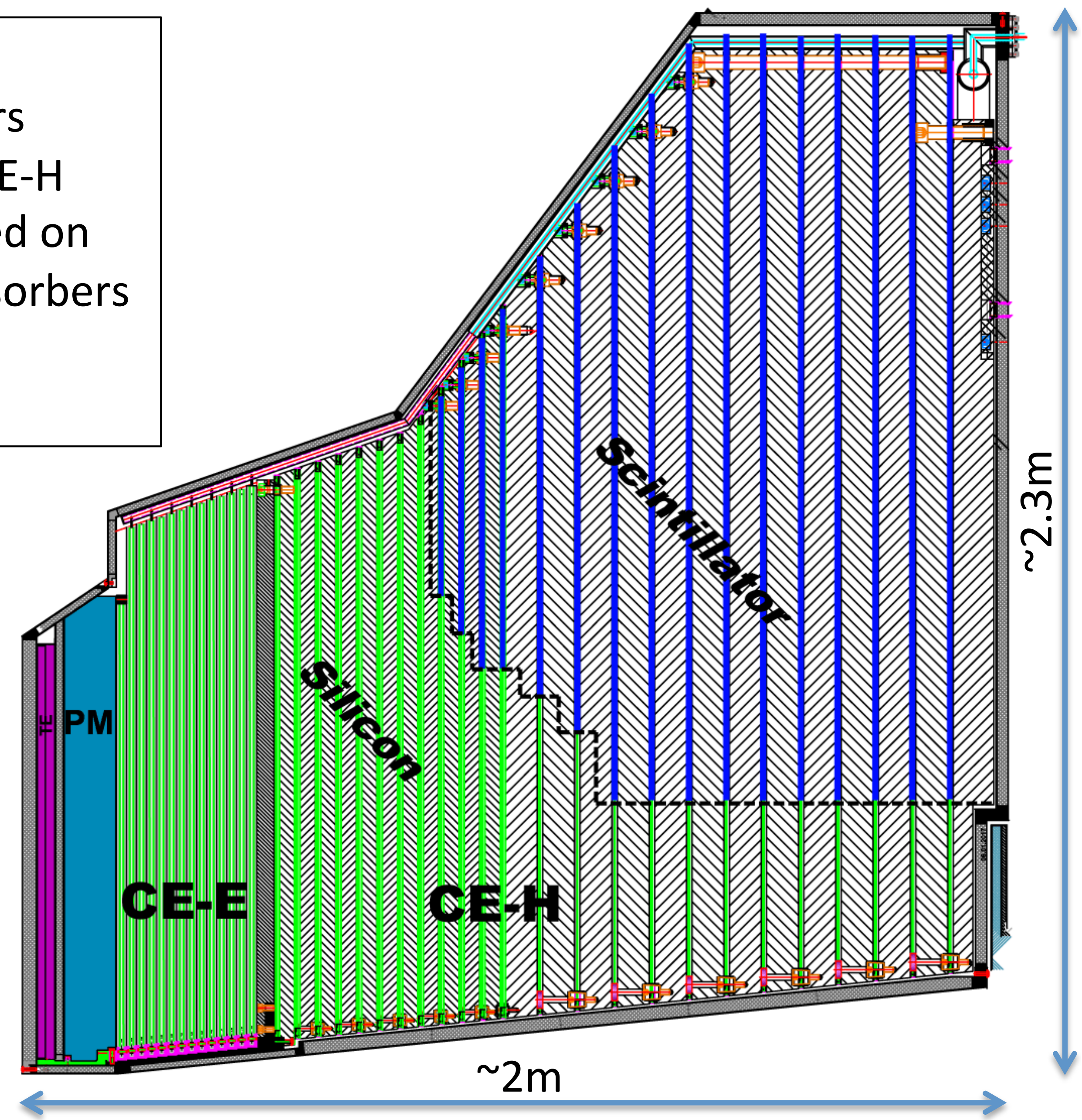

Electromagnetic calorimeter (**CE-E**): **Si**, Cu & CuW & Pb absorbers, 28 layers, 25 X_0 & ~1.3λ
Hadronic calorimeter (**CE-H**): **Si** & **scintillator**, steel absorbers, 24 layers, ~8.5λ

High Granularity Calorimeter (CE)

CERN-LHCC-2017-023

Activ
- He
  in
- "C
  co
- Sc
  lo

Key F
- CE
- ~2
- Fu
- ~6
- ~5
- 6N
- ~2
- Po
  pe

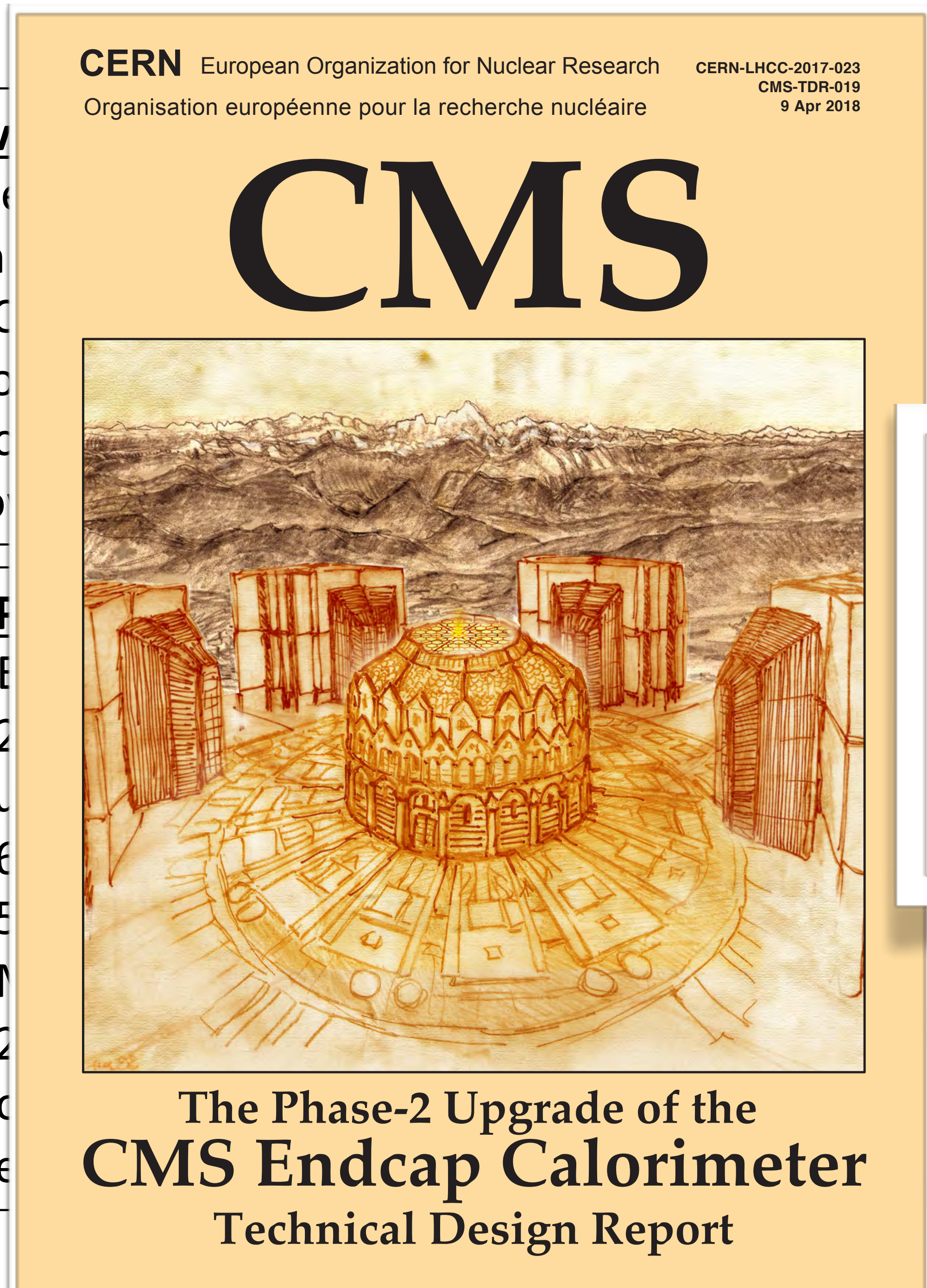

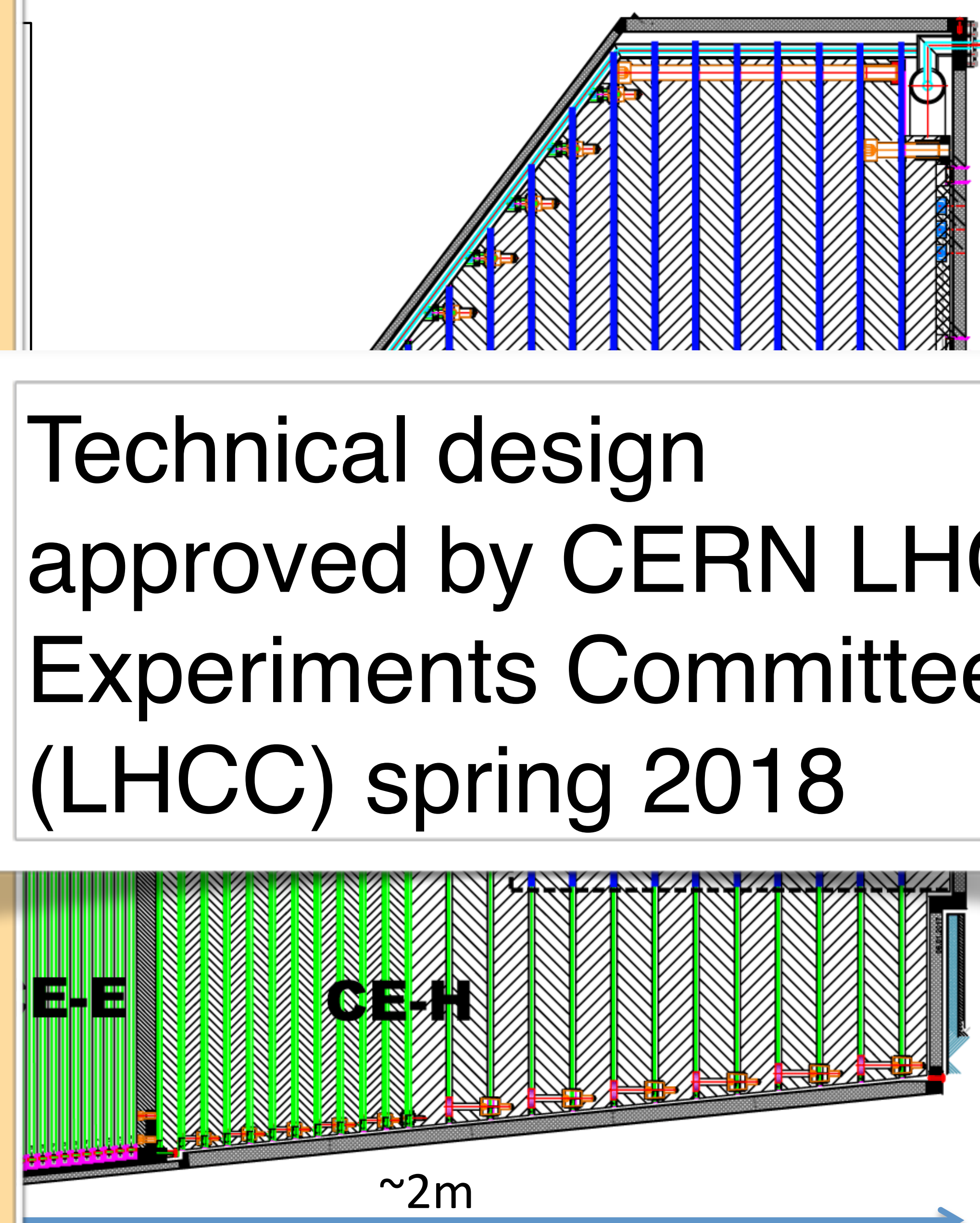

Technical design approved by CERN LHC Experiments Committee (LHCC) spring 2018

Electromagnetic calorimeter (**CE-E**): Si, Cu & CuW & Pb absorbers, 28 layers, 25 X_0 & ~1.3λ
Hadronic calorimeter (**CE-H**): Si & **scintillator**, steel absorbers, 24 layers, ~8.5λ

Design in a nutshell

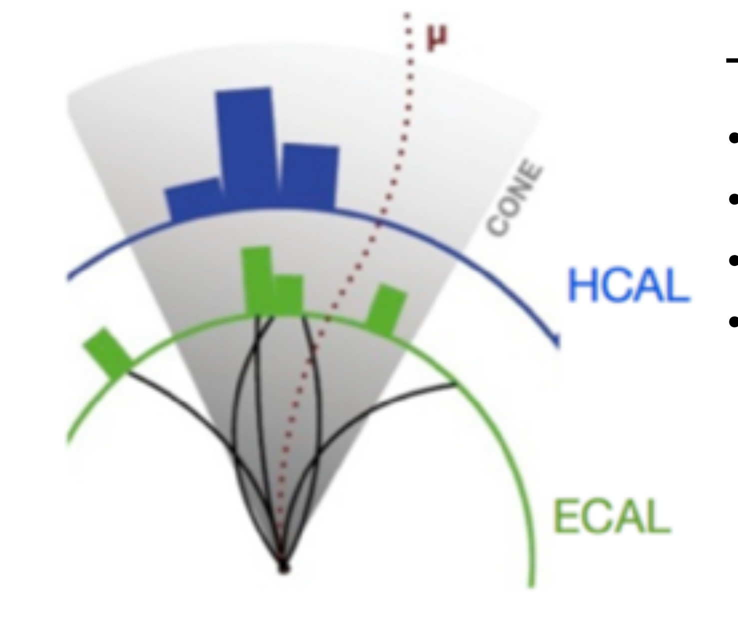

D. Barney

Typical jet is composed of:
- 62% charged particles
- 27% photons
- 10% neutral hadrons
- 1% neutrinos

JINST 12 (2017) P10003

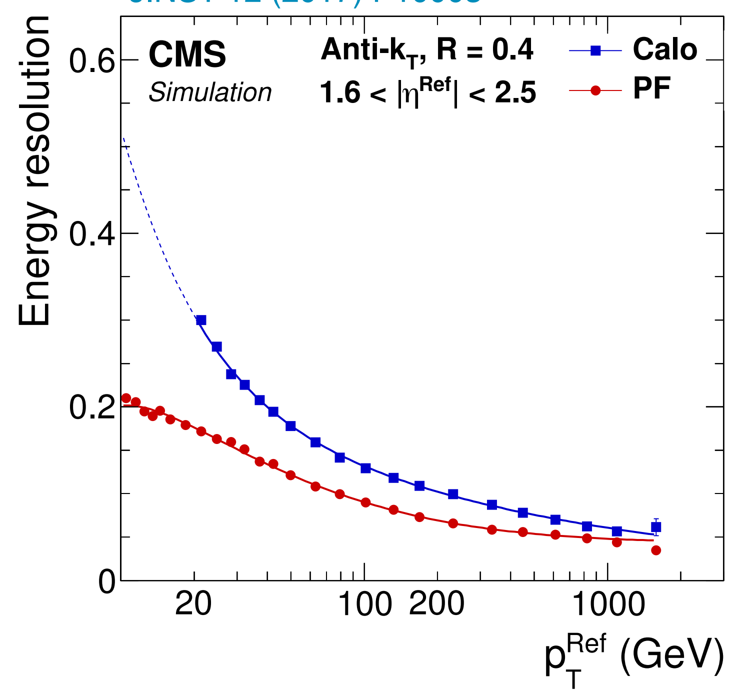

- Particle flow (PF) calorimeter, optimized for PU rejection and jet energy resolution (JER)
  - PU rejection required by high HL-LHC instantaneous luminosity
  - JER improved with respect to cone-based reconstruction
    - Good position resolution from fine longitudinal and transverse granularity to associate calorimeter segments to charged hadron tracks
    - High resolution tracking information used to estimate the energy of charged jet candidates
    - Low resolution calorimeter information “only” used to estimate the energy of neutrals

Design in a nutshell

CERN-LHCC-2017-023

Simulated MIP S/N after 3000 fb^{-1} SiPM+scintillator aging

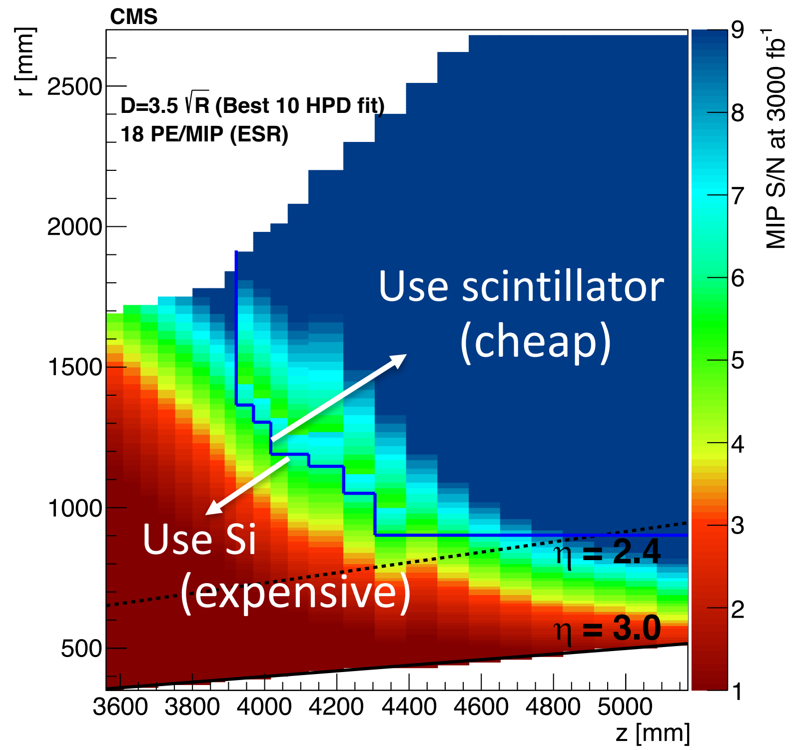

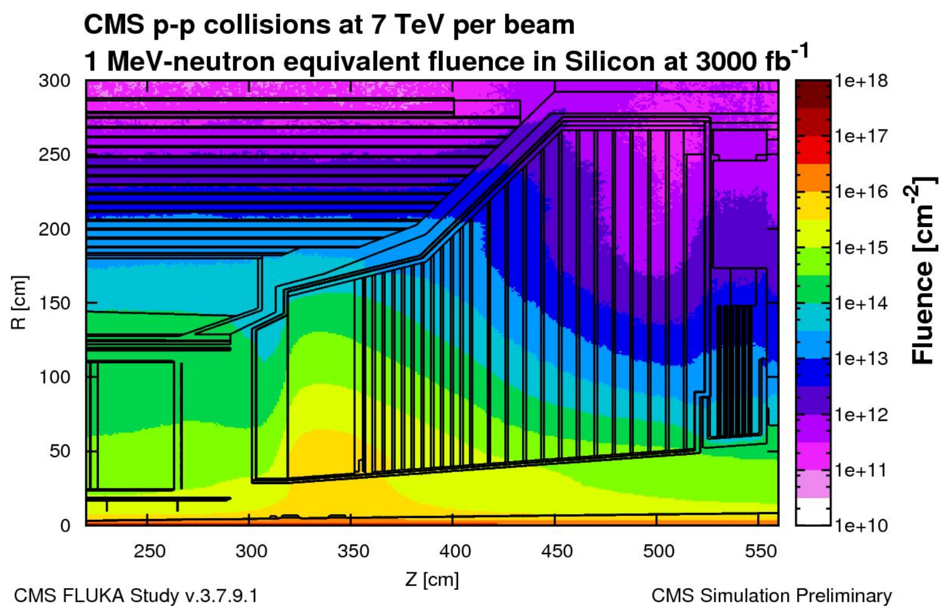

- Per-channel calibration with minimum-ionizing particles (MIPs) throughout HL-LHC lifetime imposes requirements on radiation tolerance
  - Dictates choice of active materials
  - Dictates geometry

Silicon sensor design

CERN-LHCC-2017-023

- n-on-p sensors for superior radiation hardness
- Cost optimization
  - Hexagonal sensors from 8” wafers
  - Thickness decreases as expected fluence increases
- Cell sizes (~ capacitance ~ noise) set by MIP signal-to-noise (S/N) requirement at end of life
- Threefold diamond symmetry permits easy grouping of trigger cells and association to readout chips
- Fractional variants to cover inner and outer boundaries

Active thickness (µm)	Cell size (cm^2)	Cell capacitance (pF)	Expected fluence range ($\times 10^{15}$ n_{eq}/cm^2)	Initial MIP S/N	Smallest MIP S/N after 3000 fb^{-1}
300	1.18	45	0.1-0.5	11	4.7
200	1.18	65	0.5-2.5	6	2.3
120	0.52	50	2-7	4.5	2.2

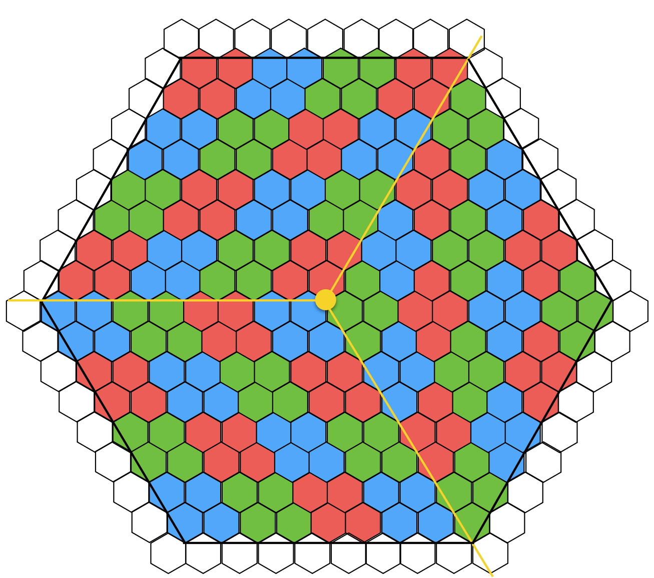
192-channel sensor

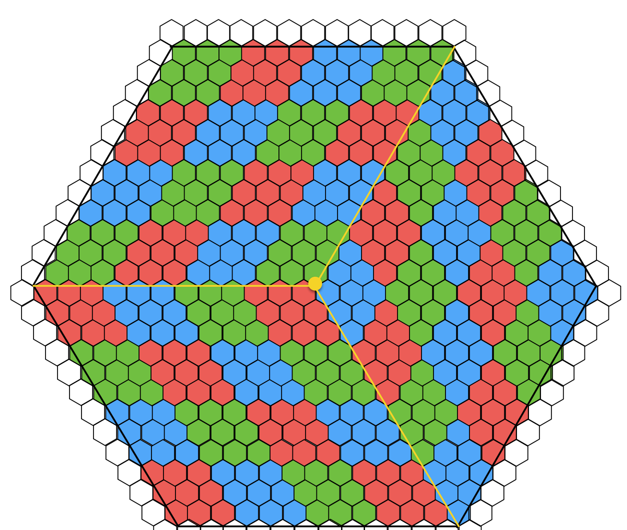
432-channel sensor

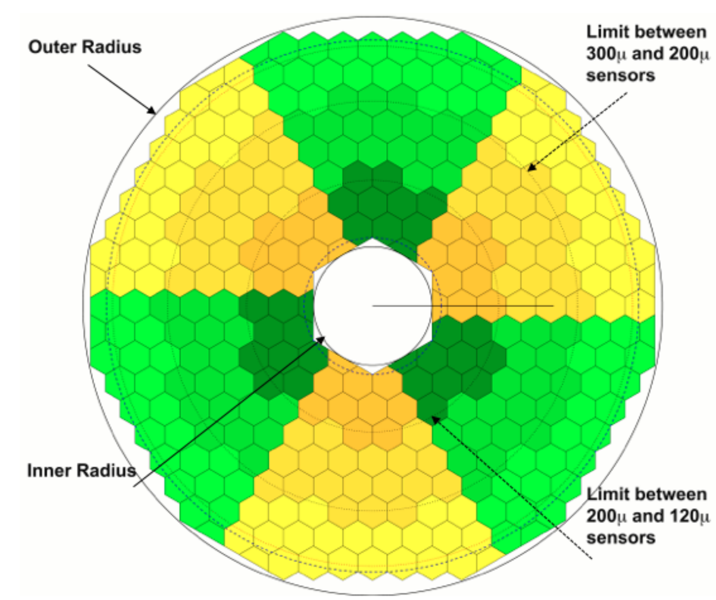

CE-E layer 9

Silicon sensor design

M. Mannelli

- 300- and 200-µm sensors in physically thinned float zone (FZ) silicon
- 120-µm sensors in epitaxial high-resistivity silicon layer on lower resistivity substrate ("epi")
- "Mouse bites" for module mounting
- Dedicated small (low-capacitance ~ low-noise) calibration cells
- Common and individual p-stops under consideration

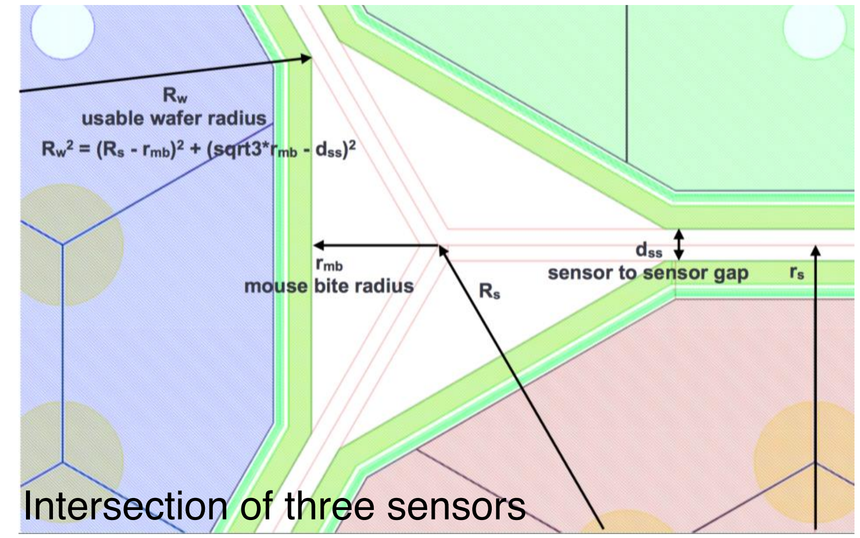

Intersection of three sensors

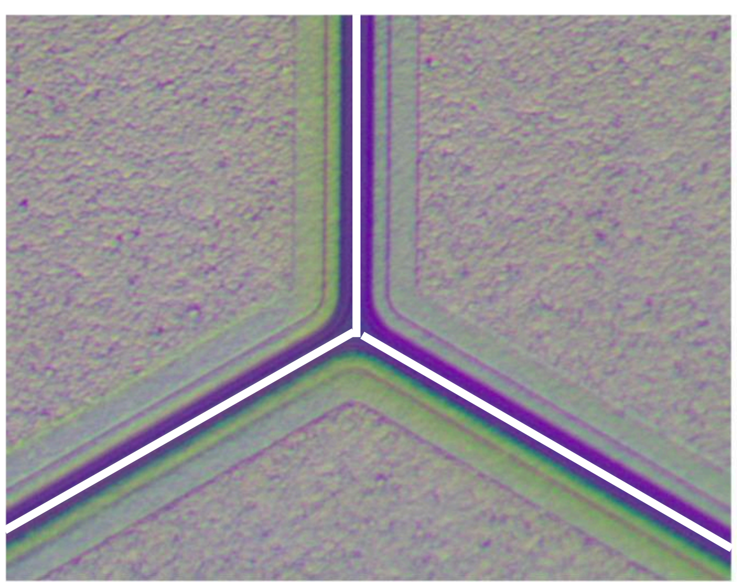

Common p-stop

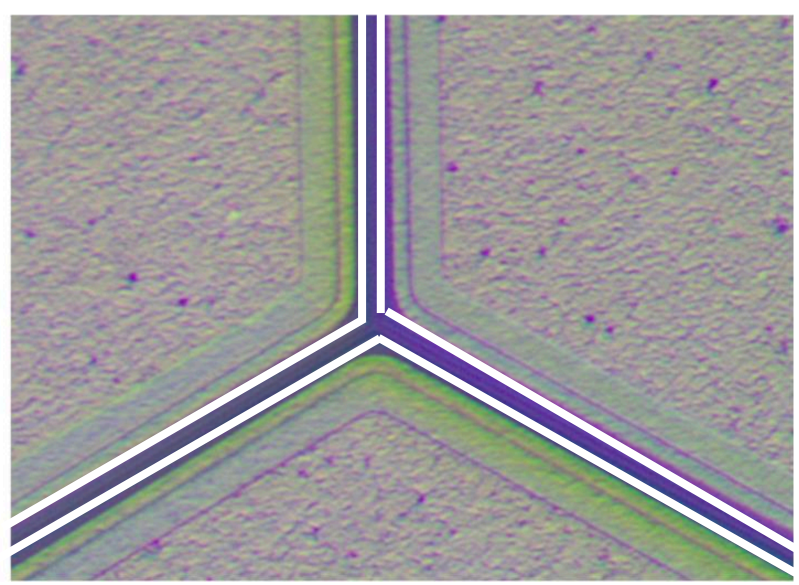

Individual p-stop

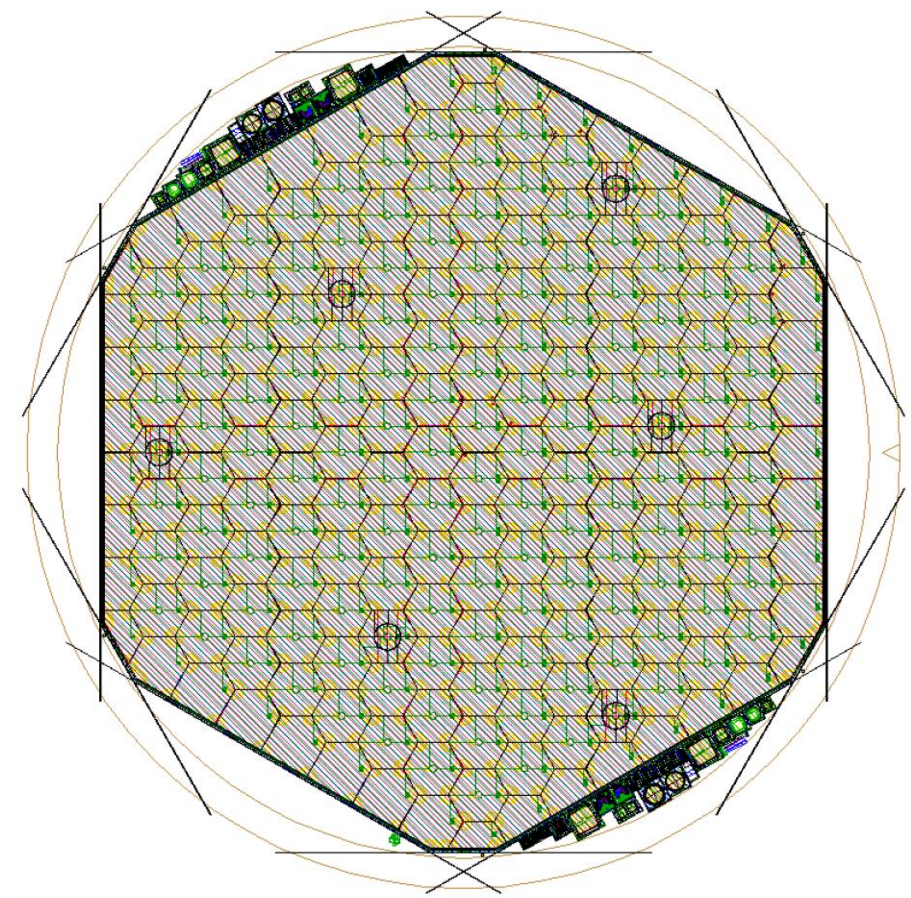

192-channel wafer layout with calibration cells

Silicon sensor prototyping

Prototyping timeline

CMS Phase 2 Tracker R&D: Hamamatsu
- FZ (200- and 320-µm) vs. epi (120-µm)
- n-on-p vs. p-on-n
- Proton (23 MeV and 24 GeV) and reactor neutron irradiation campaigns

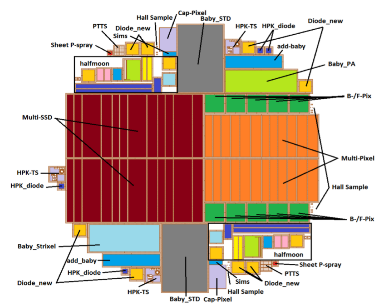

JINST 6 (2011) P10010

8” hexagonal n-on-p sensors: Hamamatsu
- FZ (300- and 200-µm) and epi (120-µm)
- 192 channels (current module design)
- Common vs. individual p-stop
- Stepper and full-wafer lithography

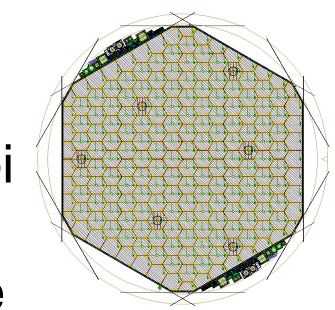

2011 2012 2013 2014 2015 2016 2017 2018 2019

CE R&D: Hamamatsu
- Test structures on Phase 2 tracker wafers
- Reactor neutron irradiation campaign

6” hexagonal sensors: Hamamatsu
- FZ (300-µm) and deep-diffused float zone (ddFZ) (200- and 120-µm)
- n-on-p vs. p-on-n
- 128- and 256-channel variants
- Common vs. individual p-stop
- Reactor neutron irradiation campaign

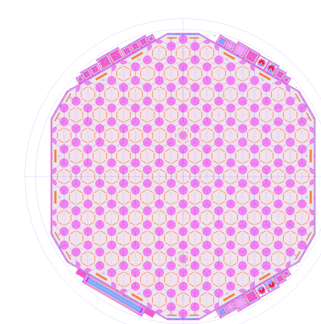

Lessons learned: tracker R&D

JINST 12 (2017) P06018

- Thin (≤300 µm) sensors required in regions of highest fluence
  - Over-depleted operation necessary for maximum charge collection
  - Reduced full depletion voltage ⇒ reduced leakage current ⇒ reduced power dissipation
- n-on-p sensors have better noise performance after irradiation than p-on-n

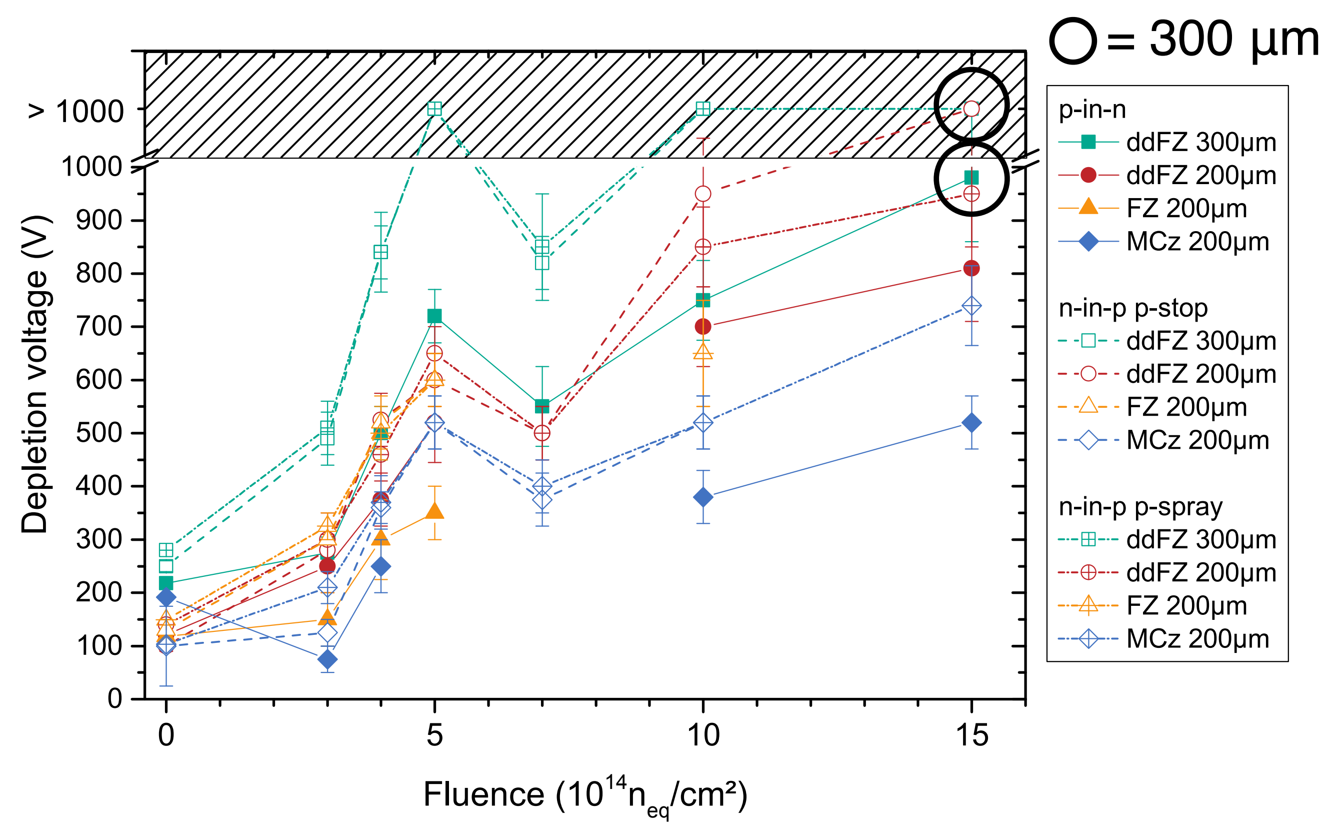

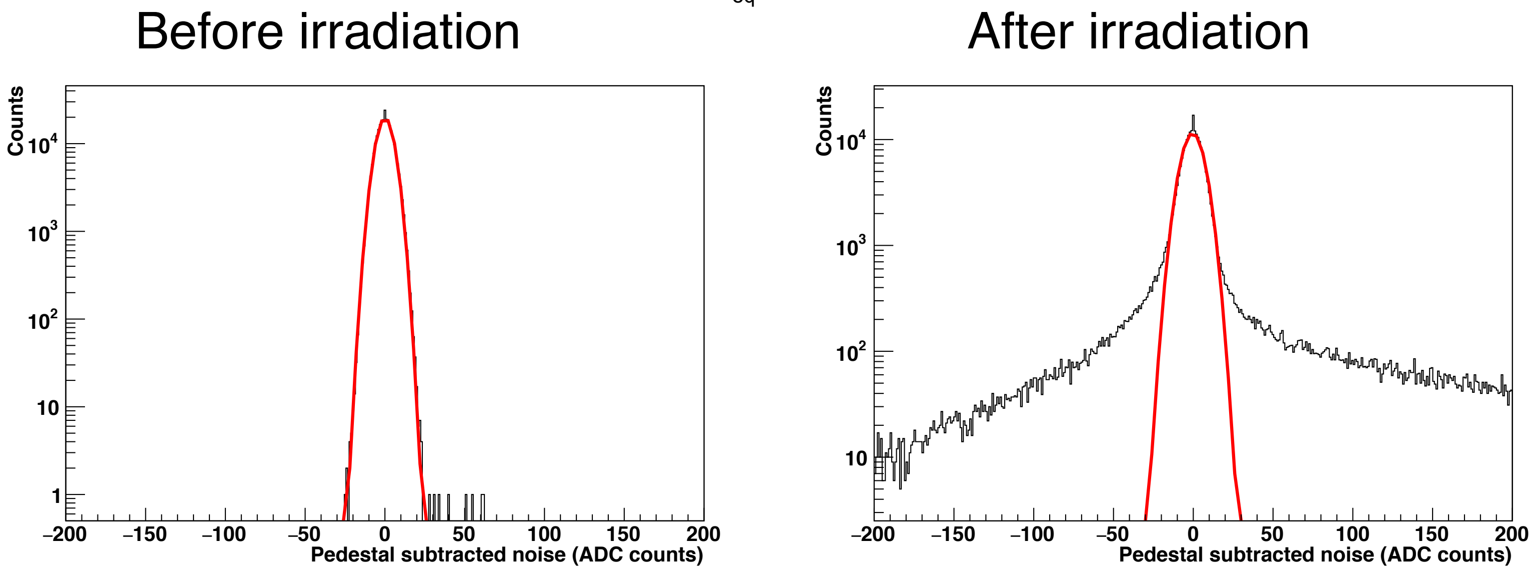

200 µm p-on-n pedestal-subtracted noise

Lessons learned: CE R&D

CERN-LHCC-2017-023

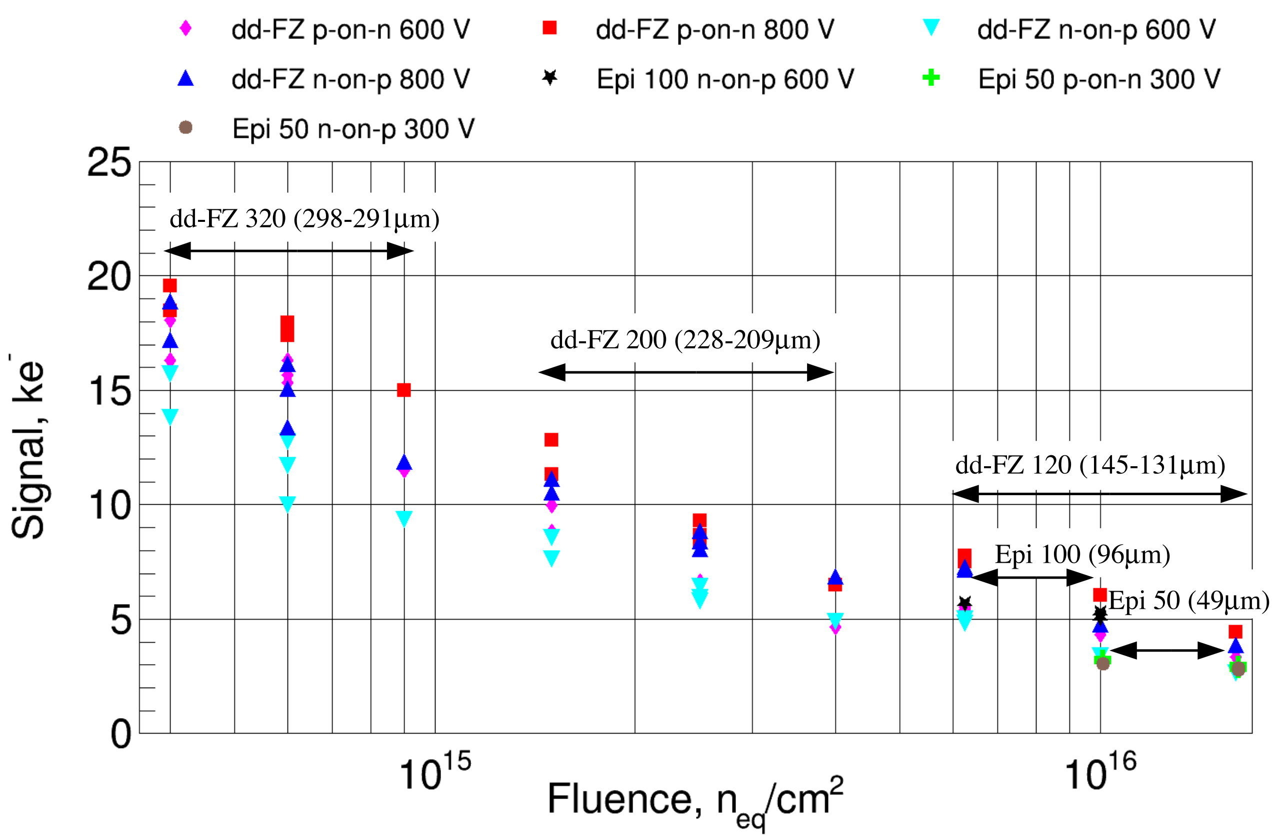

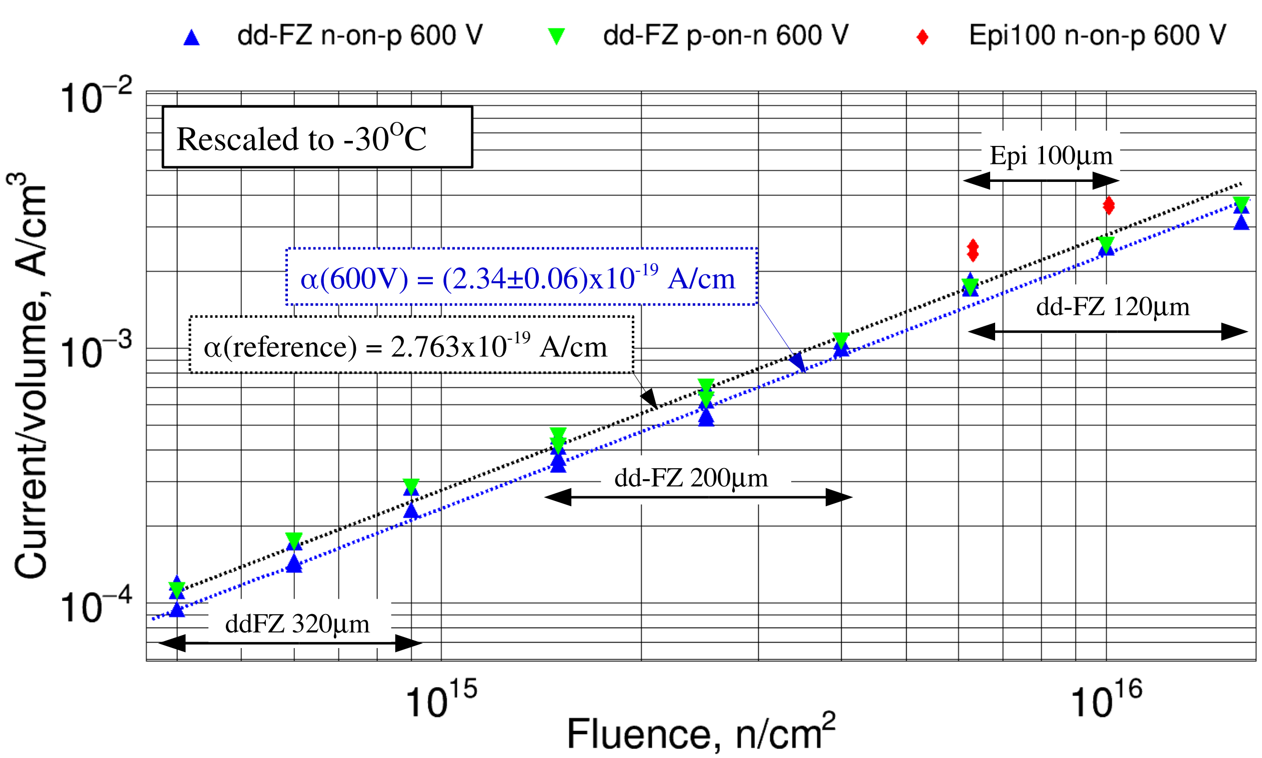

- Difference in charge collection between p-on-n and n-on-p sensors small above 10^{15} n_{eq}/cm^2
- Above ~6×10^{15} n_{eq}/cm^2, 100-µm epi n-on-p sensors (300 V bias) collect more signal charge than 120-µm ddFZ n-on-p sensors (600 V bias)
- Diode noise measurements agree with Hamburg model (linear dependence of current/volume on fluence)

Lessons learned: Hamamatsu 6”

CERN-LHCC-2017-023

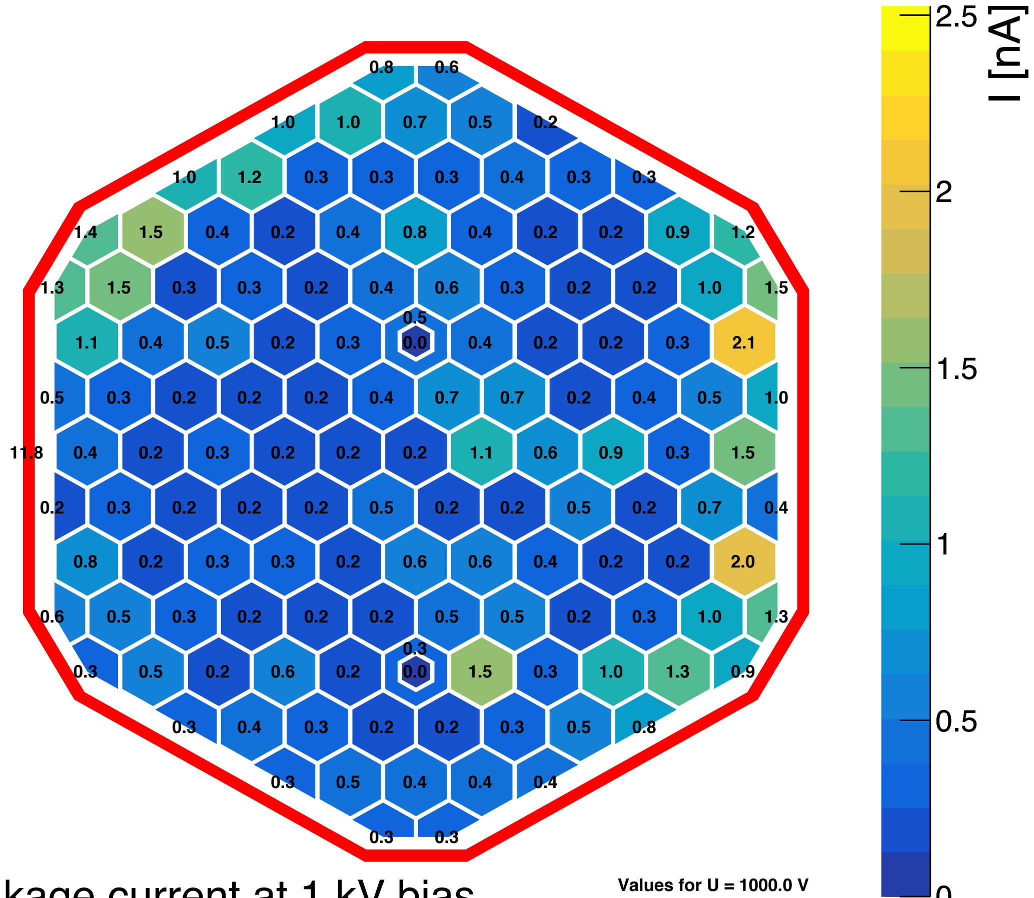

Per-cell leakage current at 1 kV bias for one 128-channel sensor

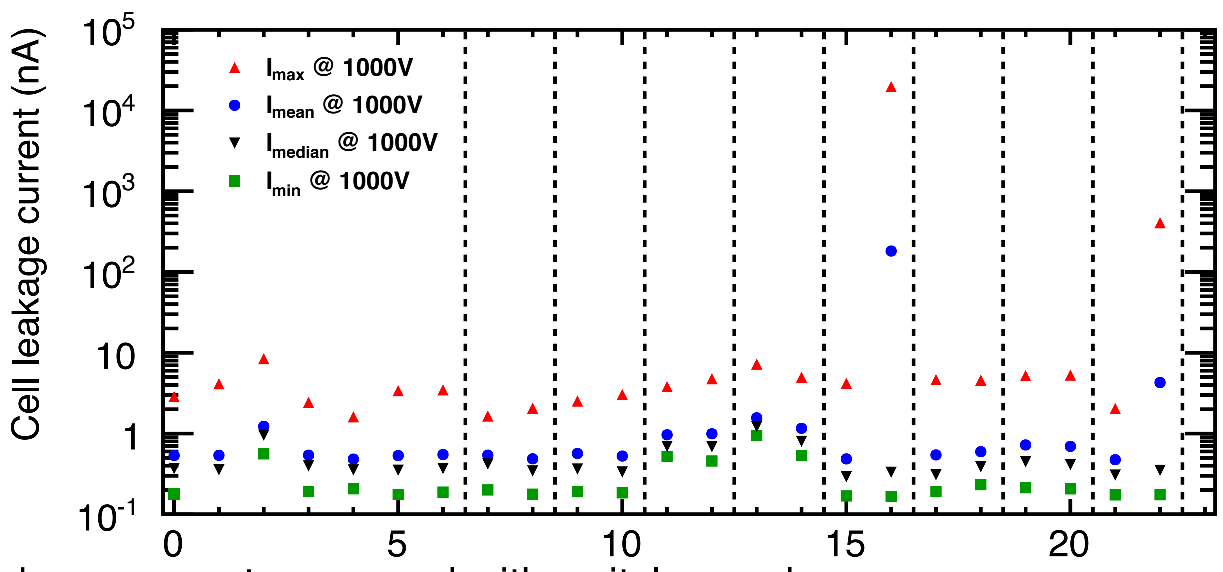

Leakage current measured with switch + probe card setup (23/200 sensors)

- Excellent sensor performance across 200 prototypes
  - Homogeneous leakage current across sensor area
  - Per-cell leakage current at 1000 V before irradiation of order 1 nA (spec is ≤100 nA per cell, ≤20 μA per sensor at 800 V and 20°C)
  - Breakdown voltage typically >1 kV
- Hamamatsu established as a reliable vendor
  - Leakage current measurements in agreement with those supplied by Hamamatsu
  - Decision made to develop 8” sensors
- Development of switch + probe card system for fast sensor characterization

Lessons learned: Hamamatsu 6”

M. Valentan

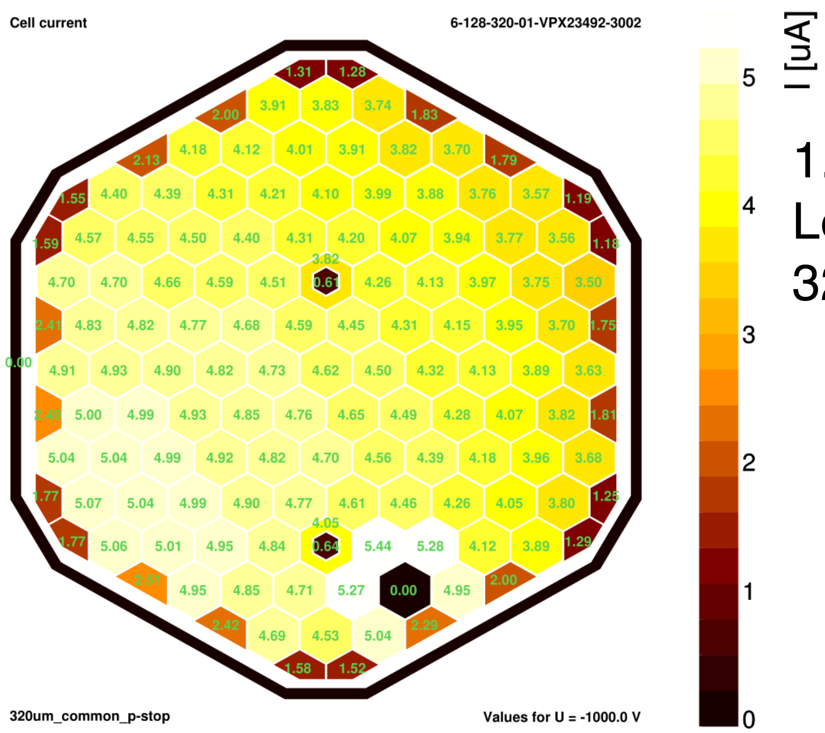

$1.5 \times 10^{14}\ n_{eq}/cm^2$
Leakage current at 1 kV
320 µm common p-stop

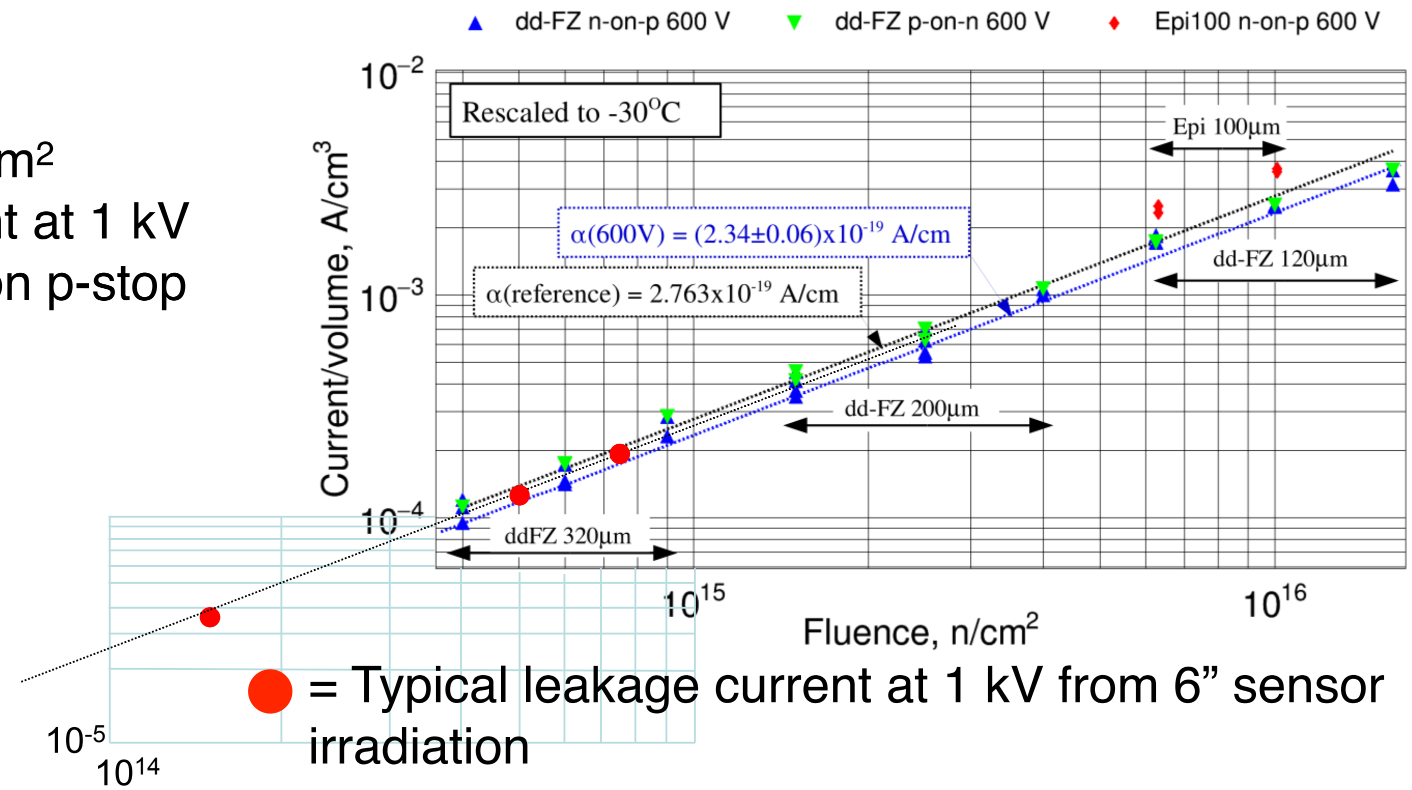

= Typical leakage current at 1 kV from 6” sensor irradiation

- Sensors exposed to 1.5-7.5 × $10^{14}\ n_{eq}/cm^2$
- Performance after neutron irradiation in line with expectations
  - Leakage current scales with cell area
  - Dependence of leakage current per unit volume on fluence agrees with Hamburg model expectation
- Noise measurements needed to confirm non-Gaussian tails in p-on-n sensors

Lessons learned: Hamamatsu 8”

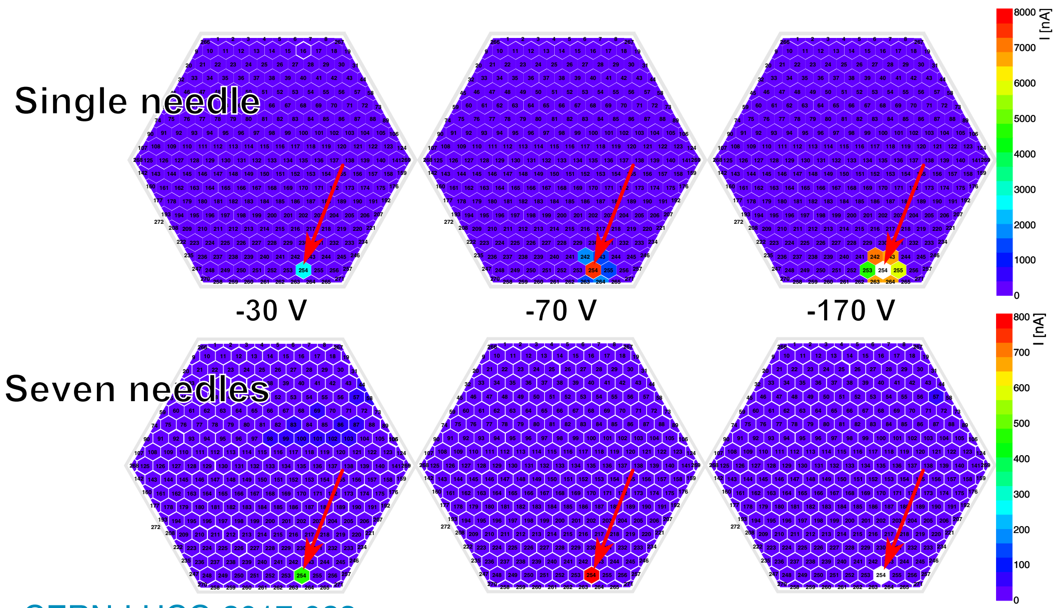

CERN-LHCC-2017-023

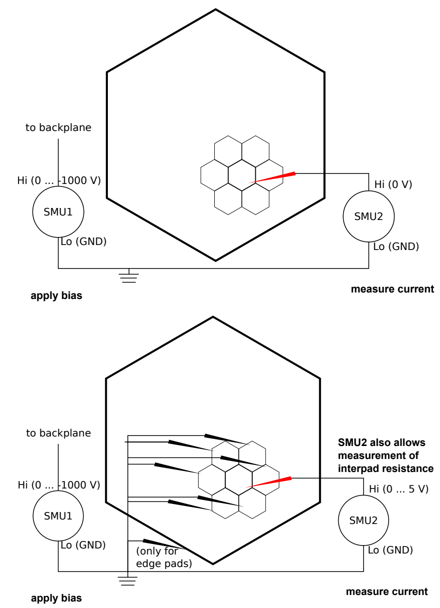

- Stepper sensors considered an 8” proof of principle for investing in full-wafer lithography
- Commissioning of different measurement techniques for quality control
  - Sensor geometry and DC coupling precludes an integrated biasing circuit with a single grounded contact point for IV and CV testing ⇒ multiple cells need to be biased simultaneously to replicate operating conditions
  - “Seven-needle” measurement as reference
  - Probe card with pogo pin contacts for fast characterization

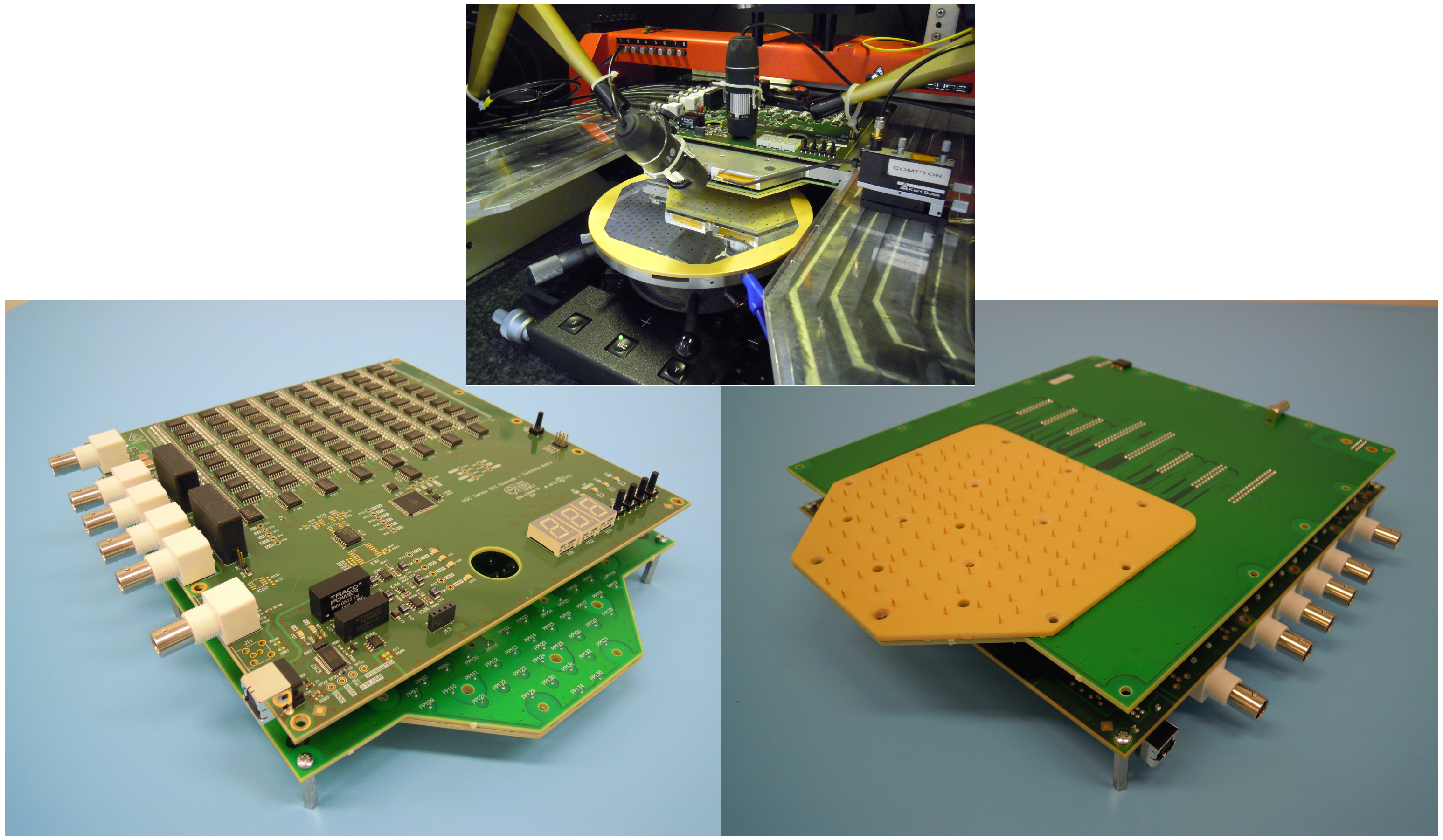

E. Sicking

Lessons learned: Hamamatsu 8”

E. Sicking

Per-cell IV curves for prototype 192-channel sensor (300 µm, individual p-stop)

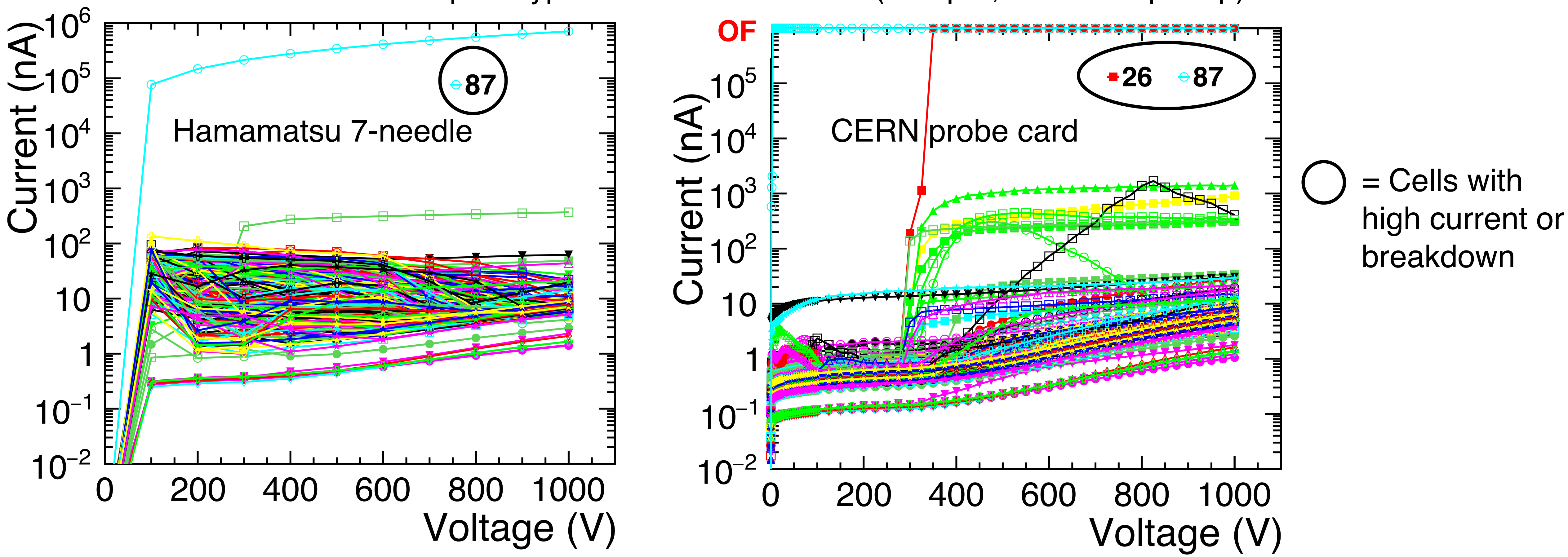

- Excellent sensor quality as for 6” sensors
- Good agreement with Hamamatsu leakage current measurements
- Per-cell capacitances in line with TDR expectation

Cell area (cm^2)	Sensor thickness (µm)	Design capacitance (pF) TDR	Measured capacitance (pF) Hamamatsu prototypes
1.18	200	65	69-71
1.18	300	45	49-50

Performance

Test beam: 2016

JINST 13 (2018) P10023

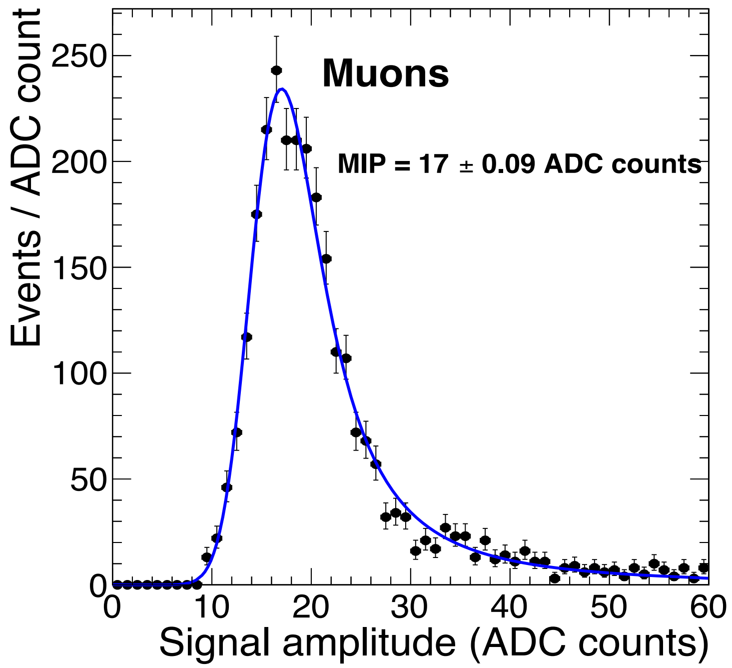

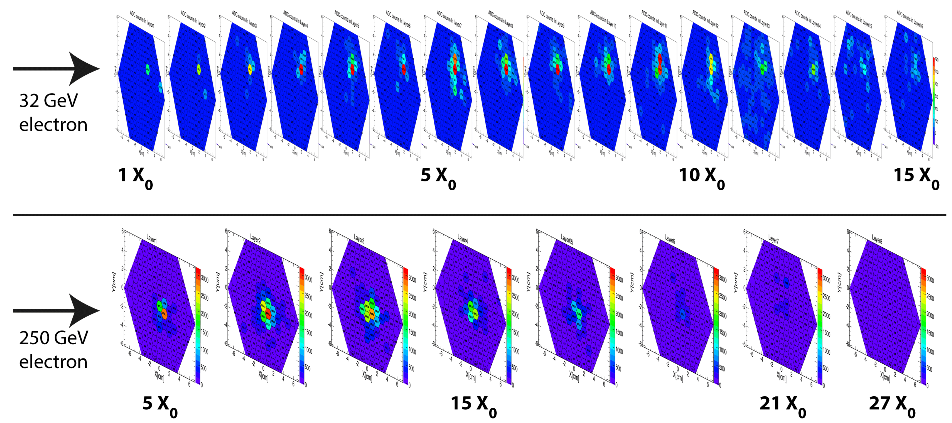

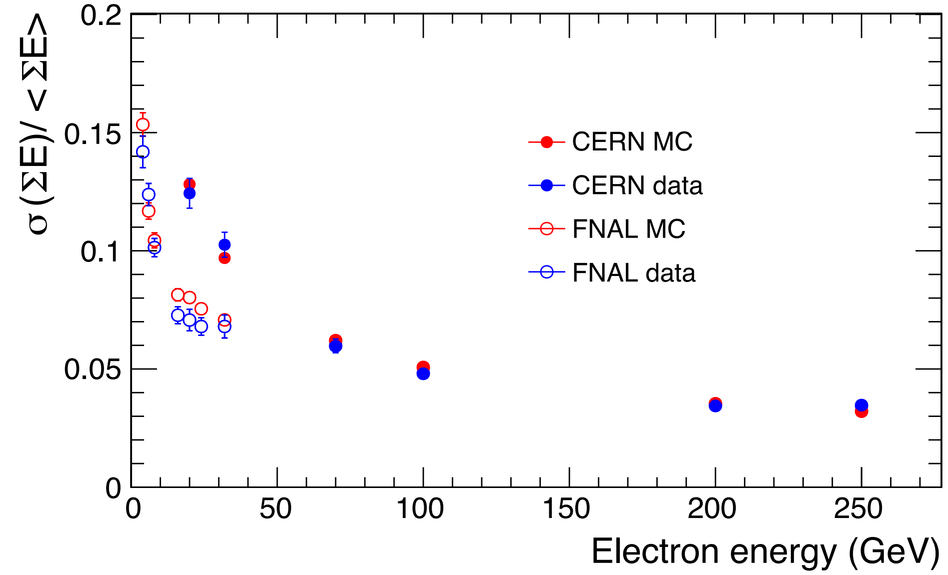

- 6” modules with different depth configurations
- First demonstrations of:
  - MIP calibration
  - Shower reconstruction
  - Time tagging core of showers
    - Resolution on time difference between neighboring cells of a sensor ~25 ps at an effective S/N of 100
    - Good timing precision can be achieved for high energy deposits found in the core of electromagnetic and hadronic showers

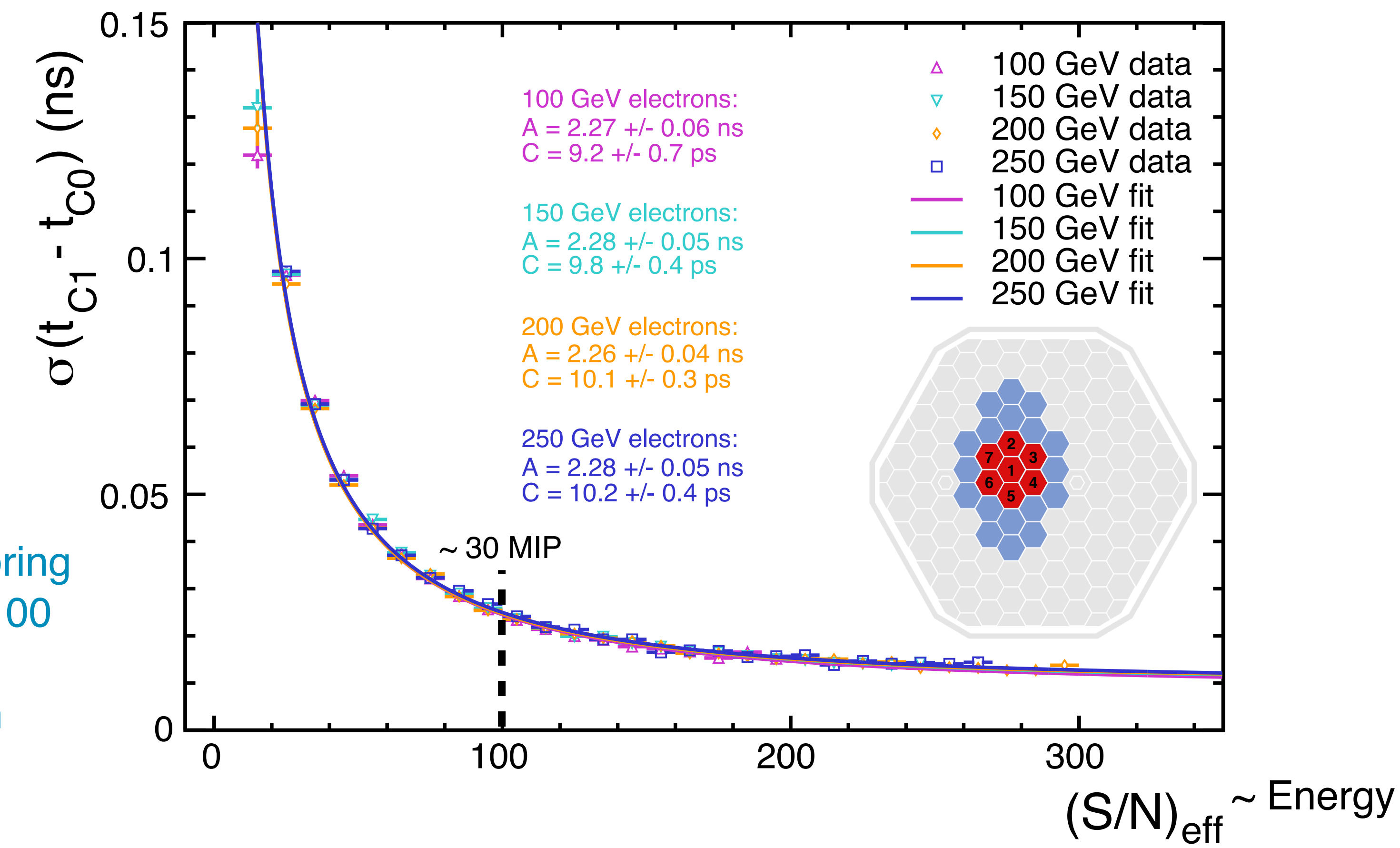

Test beam: 2018

A. Lobanov

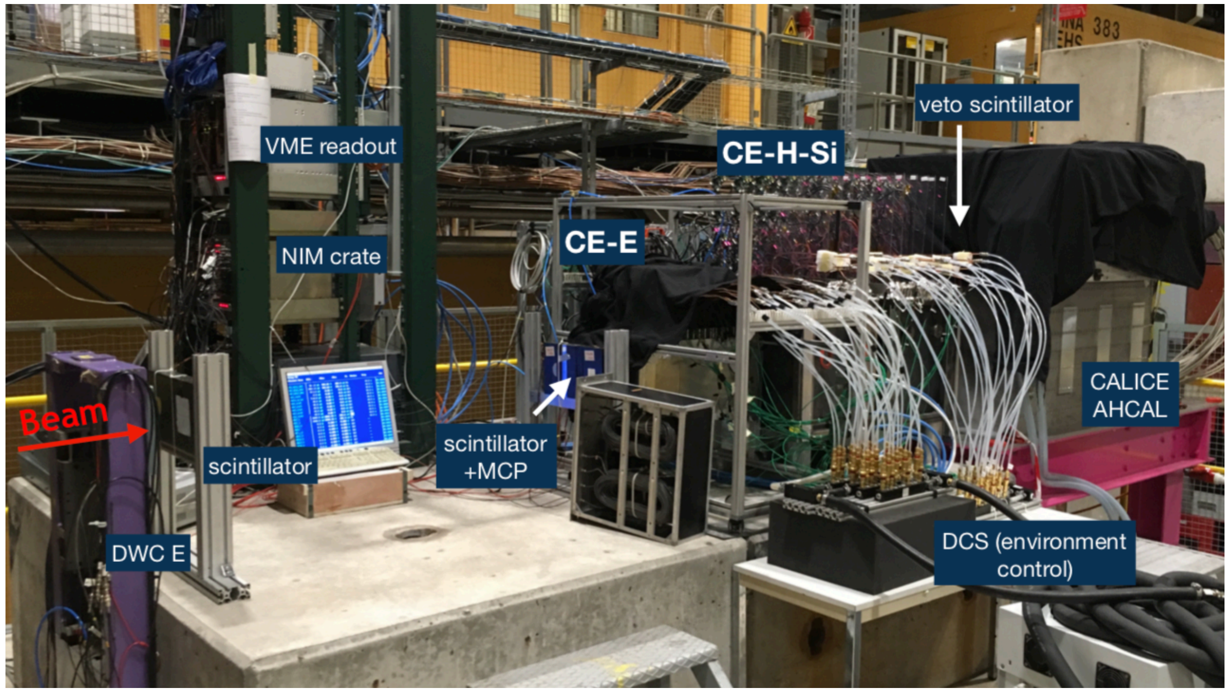

- 6” modules with readout PCB, readout chip, and absorber closer to design spec
- 28-layer CE-E + 12-layer CE-H for 94 silicon modules total (+ 39 scintillator layers behind CE-H)
- Preliminary results with basic reconstruction (currently being improved) indicate:
  - MIP signal visible even for low S/N
  - Excellent description of the energy resolution and linearity with simulation

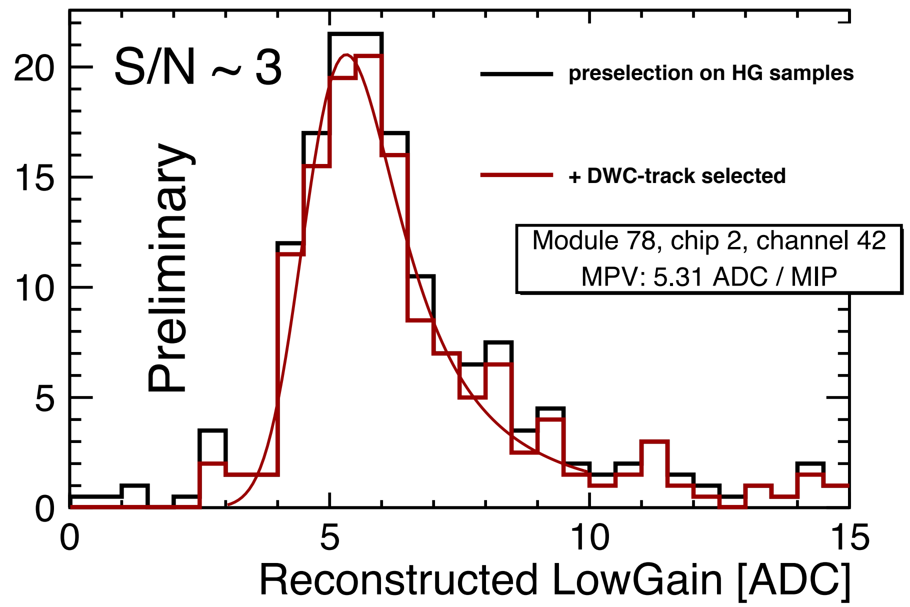

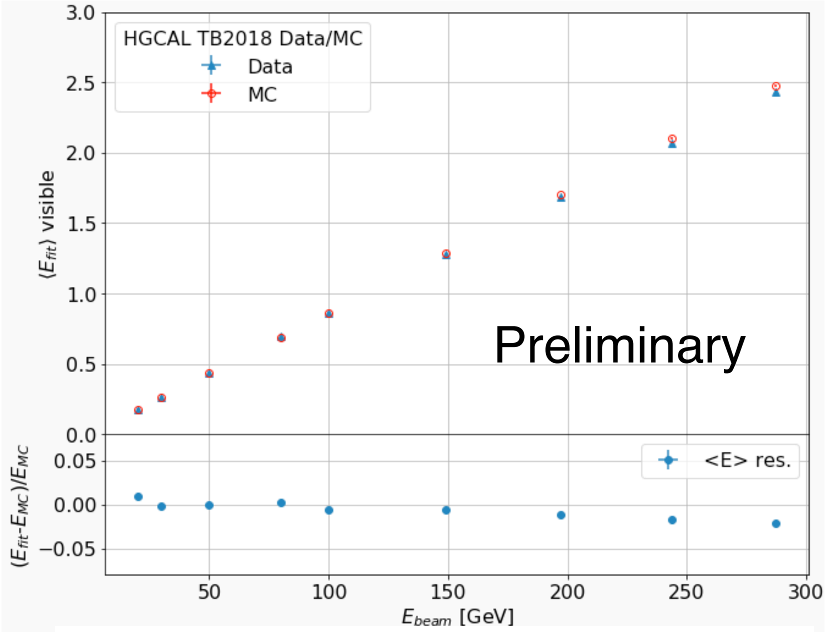

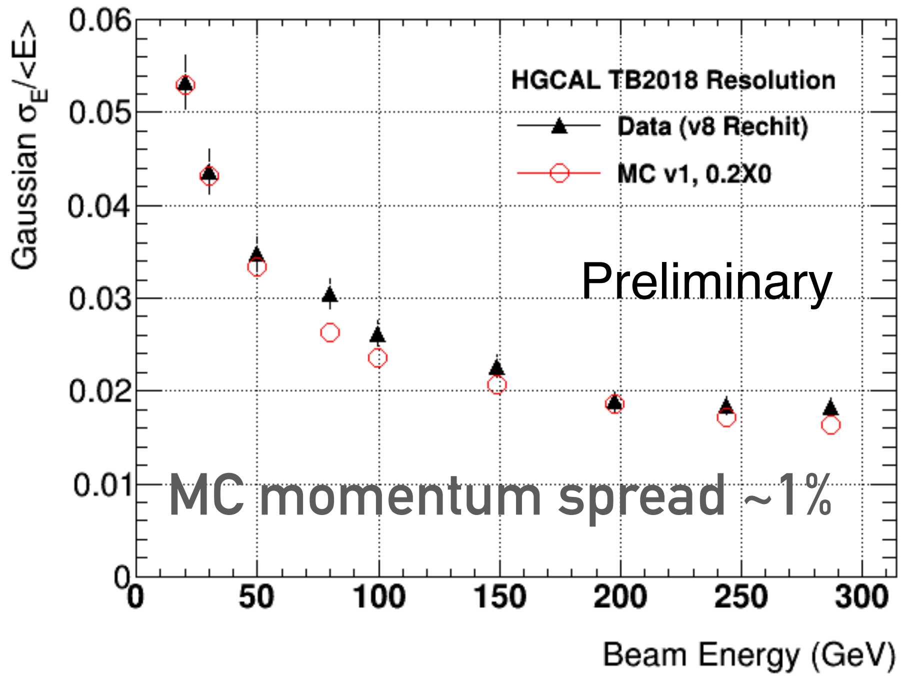

Conclusions and outlook

Sensor production schedule

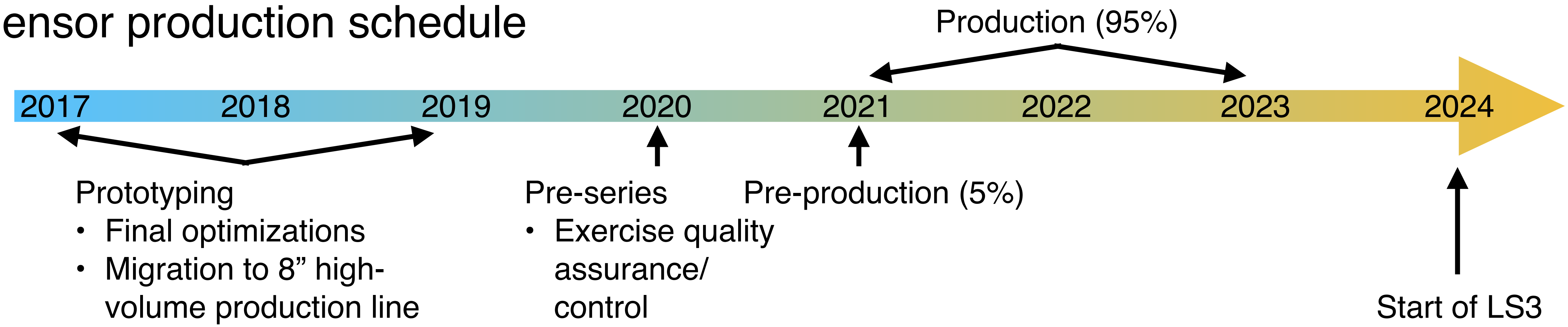

- R&D converging on an optimized, constructible design
- CE expected to play a critical role in delivering HL-LHC physics
  - PF calorimeter able to accurately reconstruct electrons, photons, taus, and jets in extremely high pileup
  - Careful deployment of active materials to ensure adequate performance after 3000 fb^{-1}
- CE a first of its kind in collider physics!

Backup

Non-Gaussian noise

CERN-LHCC-2017-023

- High electric fields between adjacent cells can create avalanche multiplication of thermally generated charge carriers
- Effect worst in p-on-n sensors with large interpad gaps (CE TCAD simulation)

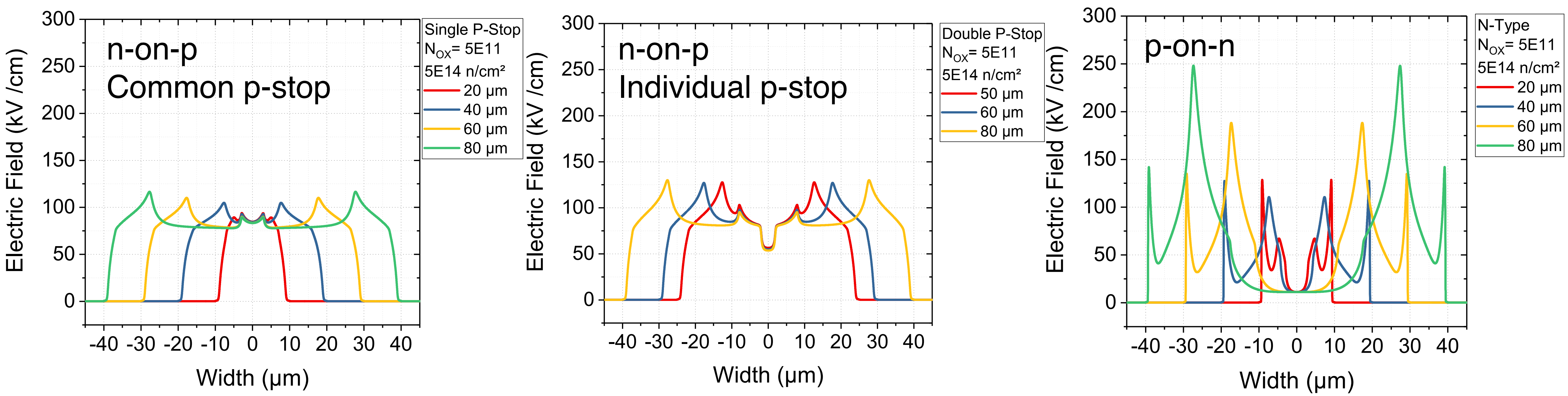

Hamburg model

M. Valentan

Current increase caused by irradiation

$$\Delta I = \alpha\, \Phi_{\mathrm{eq}}\, V$$

Temperature scaling

$$\frac{I(T_2)}{I(T_1)} = \left(\frac{T_2}{T_1}\right)^2 \exp\left(-\frac{E_{\mathrm{eff}}}{2k_{\mathrm{B}}}\left[\frac{1}{T_2} - \frac{1}{T_1}\right]\right)$$

1. Calculate current expected after irradiation
2. Scale to measurement temperature (-20 degC) and operation temperature (-30 degC)

- Parameters:
  - V = sensor or cell volume
  - Φ_{eq} = Fluence per cm² equivalent to 1 MeV neutrons
  - α = 5e-17 A/cm
  - E_{eff} = 1.21 eV (from http://iopscience.iop.org.ezproxy.cern.ch/article/10.1088/1748-0221/8/10/P10003/meta)
  - kB = 8.61733e-5 eV/K
  - $T_{reference}$ = 293.15 K (20 degC)
  - $T_{measurement}$ = 253.15 K (-20 degC)
  - $T_{operation}$ = 243.15 K (-30 degC)

Irradiated samples

Fluence (n_{eq}/cm^2)	1.5×10^{14}	5×10^{14}	7.5×10^{14}
No. sensors (300 µm p-on-n)	2	2	2
No. sensors (320 µm n-on-p common p-stop)	2	2	2
No. sensors (320 µm n-on-p individual p-stop)	2	2	2

Switch card circuit

CERN-LHCC-2017-023

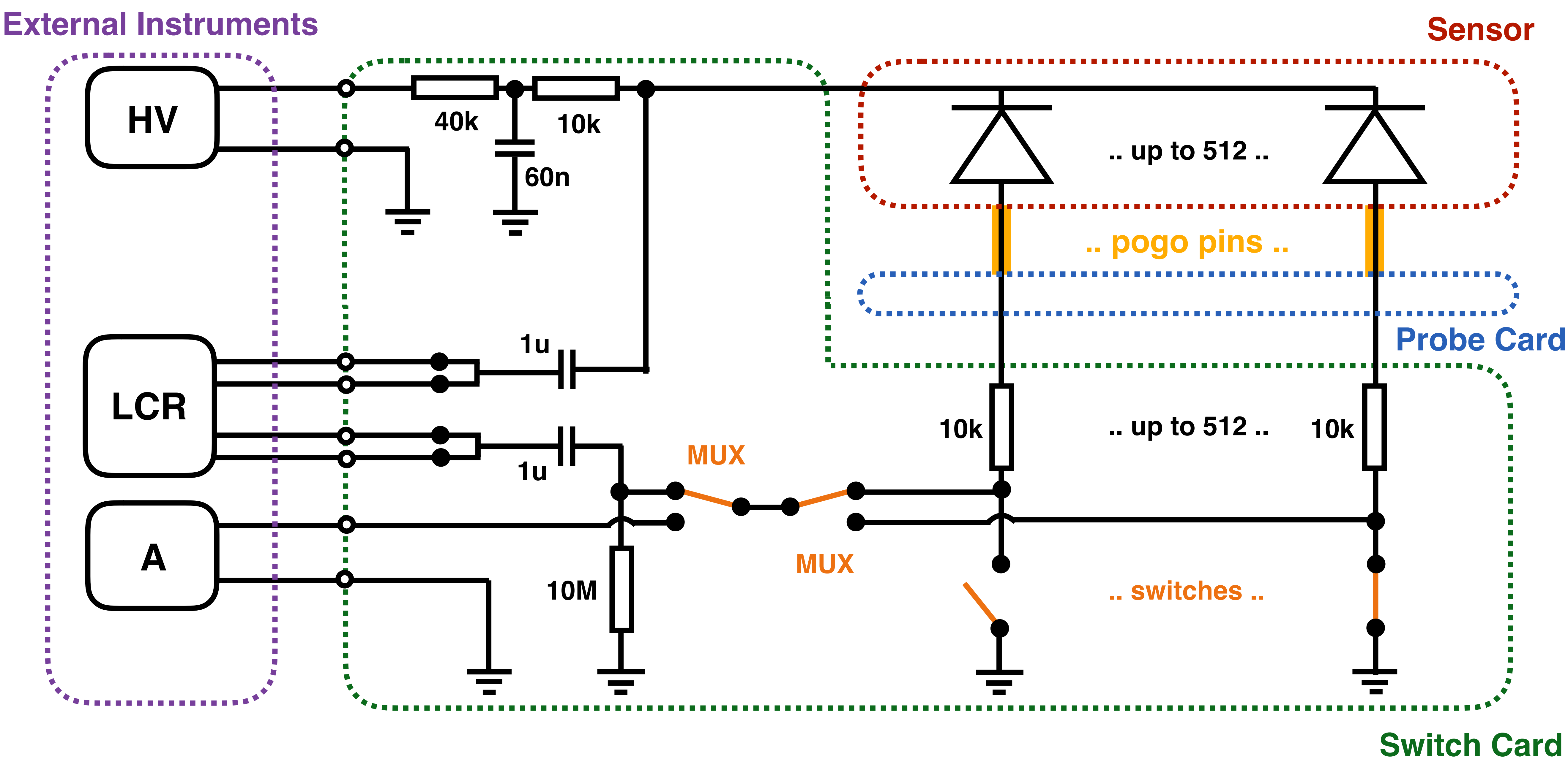

Timing resolution

JINST 13 (2018) P10023

$$(S/N)_{\mathrm{eff}} = \frac{(S/N)_{\mathrm{ref}}(S/N)_n}{\sqrt{(S/N)^2_{\mathrm{ref}} + (S/N)^2_n}}$$

$$\sigma(t_{\mathrm{ref}} - t_i) = \sqrt{\left(\frac{A}{\sqrt{(S/N)}}\right)^2 + \left(\frac{B}{S/N}\right)^2 + C^2}$$